Liquid Crystals
Publication details, including instructions for authors and subscription information:
http://www.informaworld.com/smpp/title~content=t713926090

Columnar mesomorphic properties of new macrocyclic mesogens

E. Dalcanale[ab]; A. du Vosel[a]; A. M. Levelut[c]; J. Malthéte[d]
[a] Istituto G. Donegani, Novara, Italy [b] Istituto di Chimica Organica, Università di Parma, Viale delle Scienze, Parma, Italy [c] Laboratoire de Physique des Solides, URA 0002-CNRS, Btiment 510, Université Paris-Sud, Orsay Cédex, France [d] École Normale Supérieure de Lyon, UMR 117 CNRS-ENS-Lyon, 46 Allée d'Italie, Lyon Cédex 07, France

To cite this Article Dalcanale, E. , Vosel, A. du , Levelut, A. M. and Malthéte, J.(1991) 'Columnar mesomorphic properties of new macrocyclic mesogens', Liquid Crystals, 10: 2, 185 — 198
To link to this Article: DOI: 10.1080/02678299108036424
URL: http://dx.doi.org/10.1080/02678299108036424

LIQUID CRYSTALS, 1991, VOL. 10, NO. 2, 185–198

Columnar mesomorphic properties of new macrocyclic mesogens

by E. DALCANALE*† and A. DU VOSEL*
Istituto G. Donegani, Via Fauser 4, I-28100 Novara, Italy

and A. M. LEVELUT
Laboratoire de Physique des Solides, URA 0002-CNRS,
Bâtiment 510, Université Paris-Sud, 91405 Orsay Cédex, France

and J. MALTHÊTE
École Normale Supérieure de Lyon, UMR 117 CNRS-ENS-Lyon,
46 Allée d'Italie, 69364 Lyon Cédex 07, France

(Received 26 November 1990; accepted 28 February 1991)

The mesomorphic properties of a new class of columnar liquid crystals, consisting of a bowl-shaped metacyclophane core surrounded by twelve flexible alkyl chains are reported. These mesogens form D_{ho} columnar mesophases having negative optical and dielectric anisotropy. Both planar and homeotropic alignment is obtained. An antiferroelectric pairing of the molecules within the columns is observed, ruling out the possibility of a ferroelectric self-organization of the cores. For all the mesogens a complex thermal behaviour is observed. Two different solid phases C_1 and C_2 have been characterized and their thermal behaviour elucidated: C_1 is the mesophase precursor, while C_2, more ordered, melts directly to an isotropic liquid. Mesophase stability over time depends on the length of the side chains. The overall mesomorphic complexity is attributed to the combination of the different possible core packing geometries with the numerous conformations available to the alkyl chains.

1. Introduction

Bowl-like mesogens differ from disc-like ones by their three dimensional shape and their up and down asymmetry which gives them the ability to self-organize in ferroelectric or antiferroelectric columnar arrangements [1–3]. A ferroelectric arrangement is favoured by a good stacking of the bowlic cores bringing an optimal intermolecular complementarity in shape and polarity. The first bowlic mesogens (named cone-shaped or pyramidic), already reported in 1985 [4, 5] and studied largely by X-ray diffraction [6, 7], optical microscopy [8] and deuterium NMR [7], were hexaesters of the cyclotriveratrylene core. In such mesophases, the rigid conic units may stack one on top of each other, but a finite correlation length in the column direction, measured by X-ray diffraction, reveals the existence of defects due to the inversion of the polar vector. The particular interest of these mesogens is presented by their potential ferroelectricity if all the columns are oriented in the same polarization direction (by external factors such as an electrical field or surface treatment, etc.) [9].

* Authors for correspondence.
† Present address: Istituto di Chimica Organica, Università di Parma, Viale delle Scienze, I-43100 Parma, Italy

0267-8292/91 $3·00

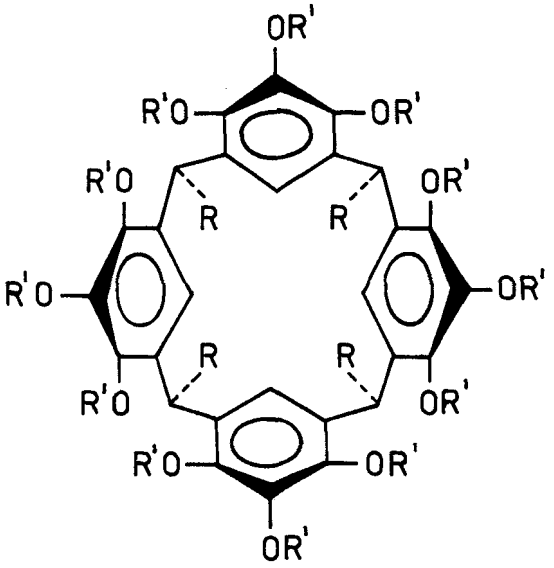

Figure 1. $R = CH_3$: (**1a–h**): $R' = -CO-C_nH_{2n+1}$; (**1a**) $n = 3$; (**1b**) $n = 9$; (**1c**) $n = 11$; (**1d**) $n = 12$; (**1e**) $n = 13$; (**1f**) $n = 15$; (**1g**) $n = 17$; (**1h**) $n = 21$; (**1i**): $R' = CO-C_6H_4-O-C_nH_{2n+1}$; $n = 12$.

In a recent communication [10] we have described the synthesis and mesomorphic properties of a new class of macrocyclic mesogens consisting of a bowl-shaped metacyclophane core symmetrically substituted by twelve flexible alkyl chains. We have shown that dodecasubstituted derivatives with sufficiently long aliphatic ester chains exhibit thermotropic columnar mesophases [11]. We report here the characterization of the mesomorphic properties of these compounds, investigated by optical microscopy, differential scanning calorimetry, X-ray diffraction and Fourier transform infrared spectroscopy.

2. Experimental

2.1. *Synthesis*

Compounds **1a–i** (see figure 1) were prepared by acid catalyzed condensation of pyrogallol with 1,1-diethoxyethane, followed by esterification of the resulting macrocyclic tetramer with the appropriate alkanoyl chloride [9–10]. All compounds gave satisfactory analytic and spectral data.

2.2. *Optical microscopy*

Thin samples were observed between two untreated cover slips of ordinary glass. The textures were studied using a polarizing microscope (Leitz, Panphot) equipped with a Mettler FP 82 hot stage. Typical optical textures were observed with little supercooling from the isotropic liquid. The thermal behaviour of mesogens **1c–g** was studied by annealing at variable temperatures.

2.3. *Differential scanning calorimetry*

DSC measurements were performed with a Perkin–Elmer DSC 7 thermal analyser. Transition temperatures and enthalpies for compounds **1a–i** depend on the scanning rate ($1°C\,min^{-1}$ to $10°C\,min^{-1}$) and on their thermal histories. Reproducible traces were obtained for all compounds during the second and subsequent heating–cooling

cycles. The results, summarized in the table, are reported for the cooling and second heating scans recorded at $10°C\,min^{-1}$.

2.4. *X-ray diffraction*

The powder diffraction patterns of unoriented mesophases of compounds **1d–g** were recorded on a Siemens D 500 TH-TH diffractometer with Ni-filtered radiation (λ_2–$K_\alpha = 1{\cdot}5418$ Å). The samples were placed in an aluminium block with a depression of ≈ 1 mm for sample containment, heated to the isotropic phase and the diffraction spectra were obtained rapidly (scan rate $= 20° min^{-1}$) upon cooling. The diffraction pattern of an aligned sample was obtained by stretching compound **1f** in the mesophase along the walls of a Lindemann glass tube. The X-ray beam was directed perpendicular to the fibre axis to obtain a section of the reciprocal space containing this axis.

2.5. *Fourier transform infrared spectroscopy*

FTIR measurements were performed with a FT-IR PE mod. 1800 spectrometer. Compound **1f** was placed between two KBr windows and heated in an electrical oven equipped with a thermocouple ($\pm 1°C$ precision). The mesomorphic behaviour of **1f** was studied as a function of decreasing temperature, starting from the isotropic liquid (82°C) to room temperature through the various phase transitions. Upon heating and annealing at 46°C the C_1–C_2 transition was analysed.

3. Results and discussion

3.1. *Thermal behaviour: DSC and optical microscopy*

Transition temperatures and enthalpy changes for compounds **1a–i**, for the cooling and the second heating cycles, are summarized in the table.

Mesomorphism is observed for the alkanoyloxy derivatives **1c–g**. Their alkoxy and benzoyloxy homologues do not exhibit liquid crystal phases. This demonstrates the importance of small modifications at the junction between the core and the chains on the organization of these compounds [11].

Benzoyloxy derivatives **1i**: substitution of the central core with twelve benzoyloxy groups gives a high temperature melting compound ($T_{CI} = 124°C$) with a low energy, sharp melting peak (see the table). Starting from the isotropic liquid a strong supercooling is observed ($T_{IC} = 68°C$, $\Delta H = 5{\cdot}5\,kJ\,mol^{-1}$).

Alkanoyloxy derivatives **1a–h**: five alkanoyloxy derivatives (**1c–g**) exhibit a mesomorphic columnar organization, detected by optical microscopy and DSC measurements. On first heating, a virgin sample obtained by evaporation of a CH_2Cl_2 hexane (4 : 1) mixture exhibits several solid–solid transitions. On further heating a highly birefringent viscous mesophase, which maintains the solid isomorphism, is observed. On rapid cooling ($10°C\,min^{-1}$) from the isotropic phase the mesophase grows with non-uniform extinction and irregularly curved boundaries or as uniform extinction domains of different directions depending on the preparation thickness. On very slow cooling, compounds **1e–g** give a fan-shaped texture typical for hexagonal columnar arrangements. Observation of a free surface preparation of **1f** confirms the uniaxiality of the mesophase, since perpendicularly oriented domains are easily obtained. It is also possible to form partially planar oriented samples by shearing them in the mesophase between two cover slips of untreated glass.

Transition temperatures (°C) and enthalpies (ΔH kJ mol^{-1}) for **1a–i** (*a*),(*d*).

Compound	Transition (*b*)	T/°C	ΔH/kJ mol^{-1}	Transition (*c*)	T/°C	ΔH/kJ mol^{-1}
1a ($n=3$)	I–C	120	21·7	C′–C	98·5	2·8
	C–C′	65·5	2·9	C–I	202	37·2
1b ($n=9$)	I–C	2	10·6	C–I	77	12·6
1c ($n=11$)	I[–D_{ho}]–C_1	52	8·9	C′–I–C_1	[59–62]	(*f*)
	C_1–C′	11	2·0	C_1–I	71	8·1
1d ($n=12$)	I–D_{ho}	58·5	10·5	C–D_{ho}	46	187·0
	D_{ho}–C	−4·5	82·5	D_{ho}–I	65·5	10·5
1e ($n=13$)	I–D_{ho}	60	10·0	C–D_{ho}	29·5	70·5
	D_{ho}–C	8	91·7	D_{ho}–I	67	12·5
1f ($n=15$)	I–D_{ho}	55·5	8·9	C–D_{ho}	48	78·0
	D_{ho}–C	27	115·7	D_{ho}–I	61	10·0
	C–C′	23·5–16·5	58·8			
1g ($n=17$)	I–D_{ho}	64·5	12·8	C–D_{ho}	58	87·0
	D_{ho}–C	38·6	145·8	D_{ho}–I	68	13·0
	C–C′	29	79·0			
1h ($n=21$)	I–C	61·5	380·7 (*e*)	C′–I–C	[76–82]	(*f*)
	C–C′	54·5	—	C–I	89	30·5
1i ($n=12$)	I–C	68·2	5·5	C–I	124·0	51·9

(*a*) These results refer to DSC measurements, 10°C min^{-1}. C, C′ and C_1: crystal forms; D_{ho}: columnar mesophase; I: isotropic liquid.

(*b*) Cooling run.

(*c*) Second heating run.

(*d*) In some cases, one or several solid–solid transitions occur at lower temperatures; the nature of C and C′ for different compounds are not correlated.

(*e*) Measured for both transitions.

(*f*) A C′–I–C–I sequence is observed: on first clearing the material immediately crystallizes into another solid form which clears again on further heating; transition enthalpies are not measurable.

The sign of the optical anisotropy, determined by introduction of an auxiliary wave plate between crossed polarizers, is negative. This is common for columnar mesophases (see figure 2). Contact preparations between compounds **1d–g** showed their complete miscibility in the mesophase region, which confirms that they belong to the same class of organization.

An interesting property of these liquid crystals is the stability of the mesophase upon addition of solvents: the columnar organization is retained up to a 30% w/w addition of benzene, that is in lyotropic conditions [12].

3.2. *Thermal history effect*

Careful optical microscopy and DSC experiments performed at slow rates (1–5°C min^{-1}) and by annealing at various temperatures have disclosed some complicated behaviour for this series of compounds: the phase behaviour depends on the heating and cooling rates and also on the thermal history of the samples. The most interesting features are

(i) all mesogens present two different crystal forms C_1 and C_2 which are precursors of respectively the mesophase and the isotropic liquid (see the scheme);

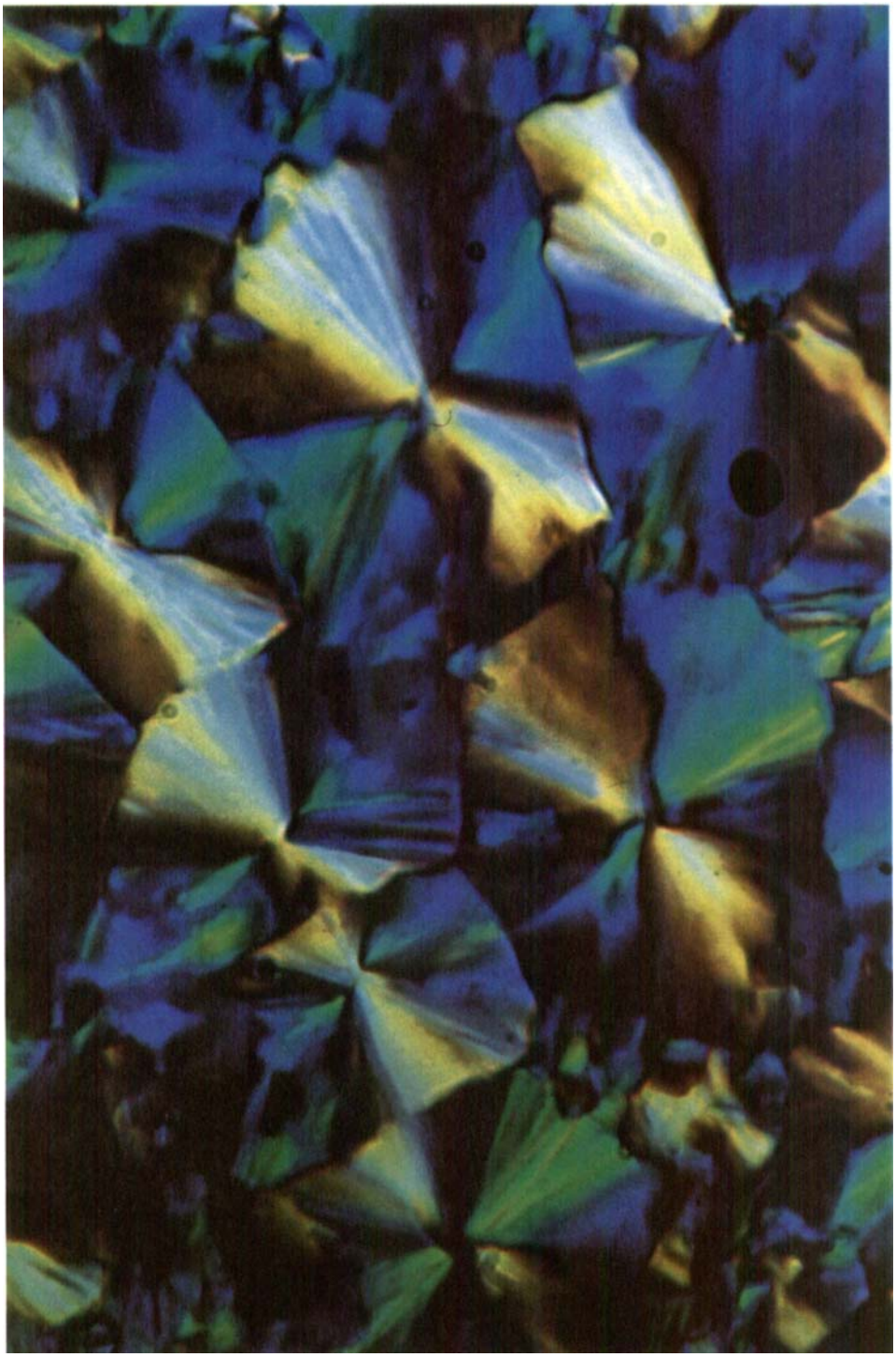

Figure 2. Photomicrograph of **1f** in its columnar phase at 60°C viewed between crossed polarizers with an auxiliary wave plate inserted.

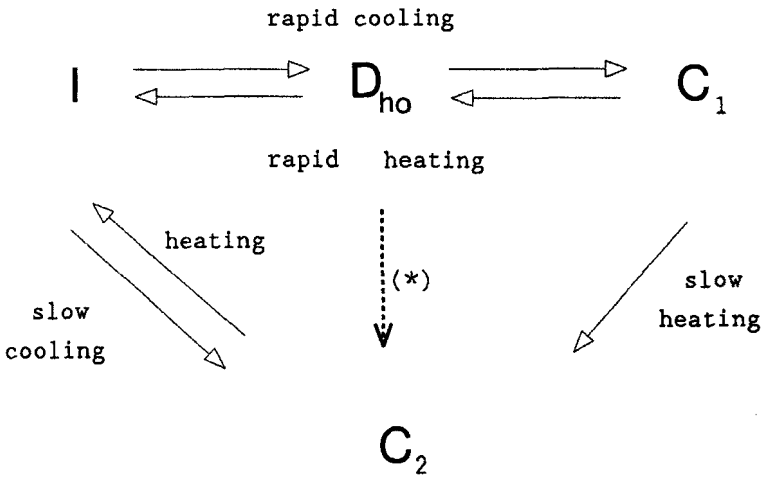

Scheme. Thermal behaviour of mesogens **1c–g**.

(ii) the mesophase stability over time increases with increasing chain length;
(iii) high homologue **1h** exhibits a double isotropic fusion: a C–I–C′–I sequence is observed

Low homologues (**1c–d**): the effects of scanning rate and of annealing time and temperature on the formation of the columnar mesophase were first shown by optical microscopy. A rapidly cooled (10°C min^{-1}) sample of **1c** from the isotropic liquid forms a mosaic-like (platelets) texture only for about 1 s, then crystallizes in a solid phase (C_1; $T_{c_1 I} = 70$°C). This transformation is clearly time rather than temperature dependent. On very slow cooling (1°C min^{-1}) from the isotropic liquid the same sample crystallizes to another solid phase (C_2, needles; $T_{C_2 I} = 75$°C). DSC traces (see figure 3) confirm the optical observations; however they measure a larger supercooling for the isotropic–mesophase transition with respect to optical microscopy, at the same cooling rate. This discrepancy results from the difference of germination between a bulky sample (DSC) and a thin layer one (optical microscopy), connected with the high order of the mesophase. In the cooling trace (10°C min^{-1}) only one peak is obtained at 52°C for both transformations: the mesophase–isotropic liquid and the C_1 mesophase transitions ($\Delta H = 8{\cdot}9$ kJ mol^{-1}). The same thermal behaviour is observed for compound **1d**: when a thin sample was rapidly cooled (10°C min^{-1}) from its isotropic state a highly birefringent texture formed at 54°C. If maintained at that temperature for about 30 min it crystallized completely in a solid phase, which probably corresponds to C_1 of **1c** ($T_{C_1 I} = 66$°C), considering their similarity in thermal behaviour and optical texture. The higher temperature melting solid C_2 ($T_{C_2 I} = 74$°C) was also observed on very slow cooling from the isotropic state (see the scheme).

High homologues (**1e–h**): mesophase stability over time readily increases in compounds **1e–g**, which still however present complex thermal behaviours. A freshly crystallized sample of **1f** ($n = 15$) exhibits three endothermic peaks for crystal–crystal (40°C), crystal–mesophase (49·5°C, $\Delta H = 276$ kJ mol^{-1} for both) and mesophase–isotropic liquid (63°C, $\Delta H = 7{\cdot}6$ kJ mol^{-1}) transitions on first heating (10°C min^{-1}, see figure 4). Upon cooling from the isotropic state, a small exothermic peak (isotropic–mesophase, 55·5°C, $\Delta H = 8{\cdot}9$ kJ mol^{-1}) is followed by crystallization peaks respectively at 27, 23·5 and 16·5°C (total $\Delta H = 174{\cdot}5$ kJ mol^{-1}). A second heating cycle shows five

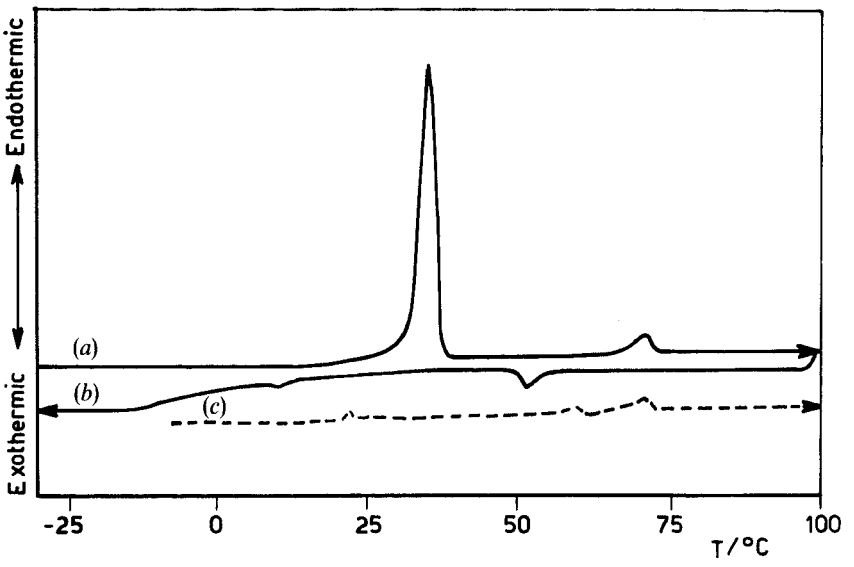

Figure 3. Differential scanning calorimetry profile for **1c**. Scan rate of 10°C min^{-1}. (*a*) First heating; (*b*) cooling; (*c*) second heating.

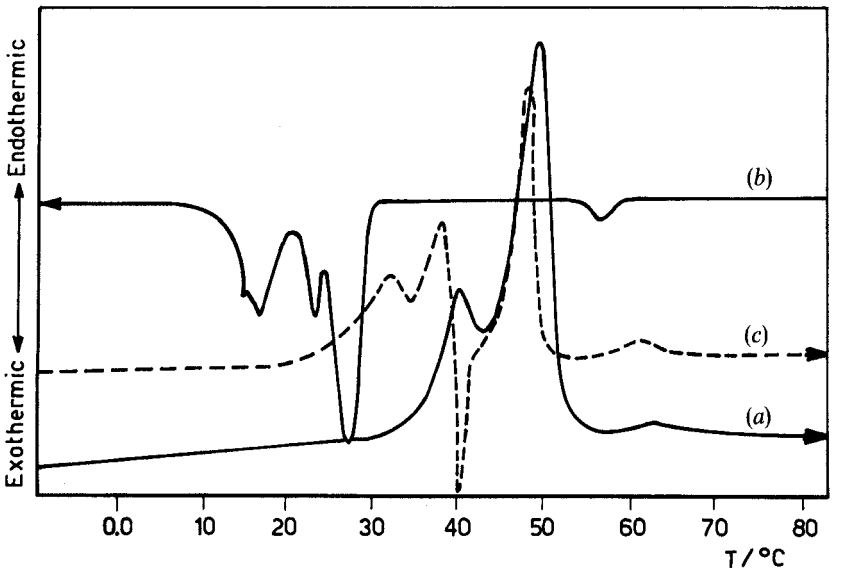

Figure 4. Differential scanning calorimetry profile for **1f**. Scan rate of 10°C min^{-1}. (*a*) First heating; (*b*) cooling; (*c*) second heating.

peaks: two crystal–crystal transitions (32 and 38°C, $\Delta H = 123$ kJ mol^{-1}) followed by an exothermic peak at $T \geqslant 39{\cdot}5$°C (a more stable phase crystallizes), a crystal–mesophase (48·0°C, $\Delta H = 78{\cdot}0$ kJ mol^{-1}) and a mesophase–isotropic (61°C, $\Delta H = 10{\cdot}0$ kJ mol^{-1}) transition.

If the mesophase is maintained at 46°C for more than three hours, a more stable and unique crystalline phase C_2 forms, which melts to an isotropic phase at 67°C ($\Delta H = 200$ kJ mol^{-1}) without proceeding to a liquid-crystalline organization (see the

scheme). Optical observations carried out under the same conditions, confirmed the slow transformation of the liquid-crystalline texture into less birefringent crystals. Annealing experiments at $T \geqslant 46°C$ showed the temperature dependence of the mesophase stability: at 57°C the mesophase is stable for more than 8 hours.

Compound **1g** ($n=17$) behaves like **1f**: at 58°C the mesophase crystallizes very slowly in the more stable solid C_2 (m.p. 78·5°C), but at 65°C it is stable for more than eight hours as confirmed by optical microscopy. Derivative **1e** ($n=13$) reveals a simpler thermal behaviour and a more stable mesomorphic state. A crystallized sample shows two endothermic peaks on heating, corresponding to the crystal–mesophase (45°C, $\Delta H = 269{\cdot}5\,kJ\,mol^{-1}$) and mesophase–isotropic (67°C, $\Delta H = 13{\cdot}8\,kJ\,mol^{-1}$) transitions. Upon cooling the mesophase–isotropic and crystal–mesophase transitions are recorded respectively at 60°C ($\Delta H = 10{\cdot}0\,kJ\,mol^{-1}$) and 8°C ($\Delta H = 91{\cdot}7\,kJ\,mol^{-1}$). The second heating trace shows a crystal–crystal transition peak at 17°C, followed by an exothermic one at $T \geqslant 19°C$, crystal–mesophase (29·5°C) and mesophase–isotropic (67°C, $\Delta H = 12{\cdot}5\,kJ\,mol^{-1}$) transitions (see figure 5). Annealing at 21°C for 30 min allows elimination of the exothermic phenomena without significant variations of the remaining transitions. When the aliphatic chains become very long (**1h**, $n=21$) the liquid-crystalline phase is suppressed. Upon cooling from the isotropic liquid two large peaks for crystal–isotropic (61·5°C) and crystal–crystal transitions are recorded (54·5°C, $\Delta H = 380{\cdot}7\,kJ\,mol^{-1}$ for both). The second heating scan shows a complex sequence of endo- and exothermic transformations: a crystal–crystal transition at 71·5°C ($\Delta H = 234{\cdot}5\,kJ\,mol^{-1}$), a crystal–isotropic transition at 76·5°C followed by an exotherm (iso-crystal) at $T \geqslant 79°C$ and finally an endotherm (crystal–isotropic) at 89°C. Formation of this double fusion sequence was confirmed by optical observations.

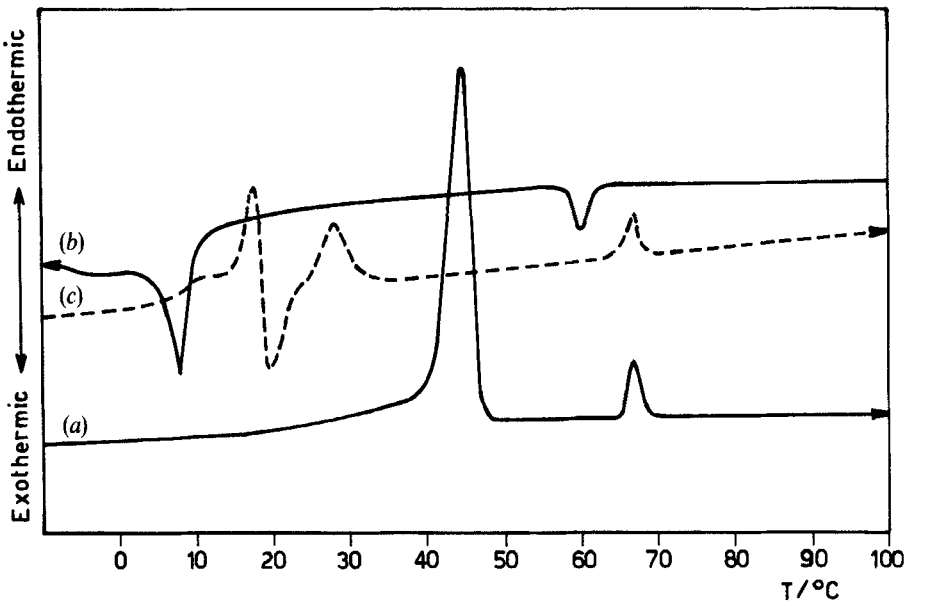

Figure 5. Differential scanning calorimetry profile for **1e**. Scan rate of $10°C\,min^{-1}$. (*a*) First heating; (*b*) cooling; (*c*) second heating.

3.3. *Mesophase characterization: X-ray diffraction and FTIR*

X-ray diffraction measurements: the powder diffraction patterns of unoriented samples of compounds **1d–g** cooled rapidly from the isotropic phase ($>10°C\,min^{-1}$) showed three areas of diffraction: a sharp, low angle peak ($2\Theta = 2–3°$), a mid angle region peak ($2\Theta = 8–9°$) and a broad feature at high angle ($2\Theta = 19–20°$). The X-ray data show that the position of the small angle reflections depends linearly on the length of the aliphatic chains (see figure 6), which shows a high degree of disorder (1·2 Å/CH_2 increase compared with the calculated 2·5 Å/CH_2). In the solid form obtained by rapid cooling from the mesophase the same organization was maintained with only an additional positional order in the columns evidenced by an intense diffraction peak at $d = 4·2$ Å. In the isotropic phase two broad, diffuse peaks remained: the typical peak of liquid alkanes ($d = 4·5$ Å) and a small one at low angles corresponding to the average molecular dimension ($d = 29·5$ Å for **1f**).

Further information on the molecular organization of the mesophase was attained on aligning a sample of compound **1f** by stretching it along the walls of the tube. In this way it was possible to obtain a perfectly aligned sample that maintained the orientation below 58°C. The column axis is parallel to the stretching direction. Two sharp spots are seen in the equatorial plane with lattice spacings proportional to 1 and $1/\sqrt{3}$, the latter has a very weak intensity. Therefore the two dimensional network of parallel columns is confirmed to be hexagonal with a lattice constant a of 36·1 Å. The outer diffuse ring

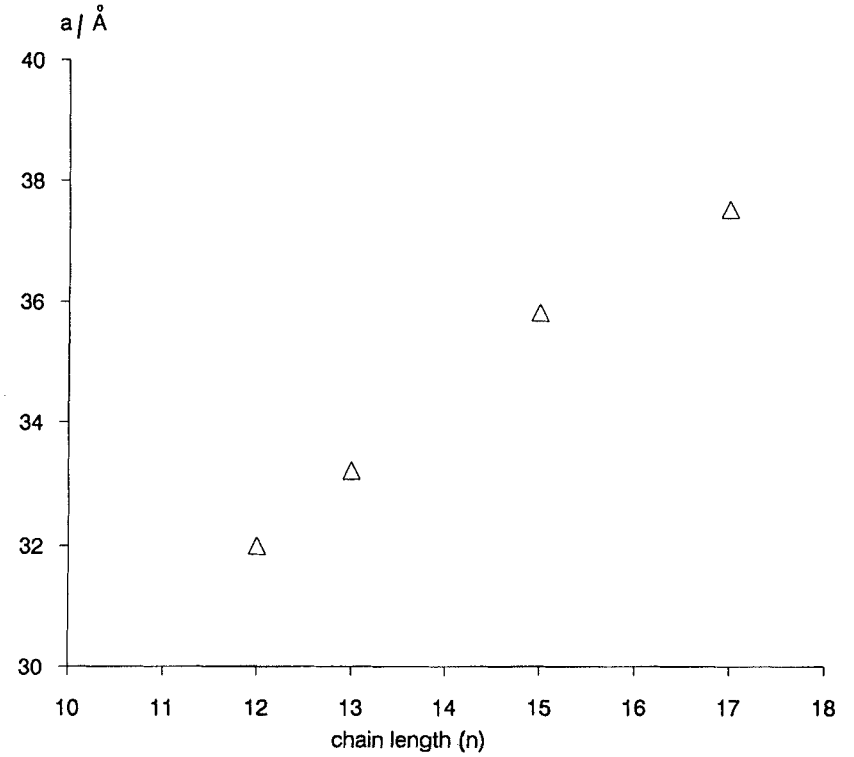

Figure 6. Distance values (calculated from the lowest angle peak) versus chain length for **1d–g** samples cooled rapidly ($>10°C\,min^{-1}$) from the isotropic phase.

($2\Theta = 19$ Å) corresponds to the scattering of the aliphatic chains in a very disordered, cylindrically distributed state.

A rather diffuse line is seen in the meridian direction and it is extended in a direction perpendicular to the column axis. Therefore this diffuse line, corresponding to the inner diffuse ring seen on the powder pattern, comes from the diffraction by a periodic linear modulation along the column axis, with a period of 11·2 Å. The correlation length is at least seven times this period. This modulation could be interpreted in terms of a pairing of molecules along the columns (a specific gravity of 0·9 g cm^{-3} is consistent with a pairing of molecules along the column axis) in an antiferroelectric mode. A second explanation, as proposed by De Gennes for disc-like mesogens [13], should be the existence of a mismatch between the equilibrium distances resulting from one hand to the steric hindrance between cores and on the other hand to the optimum density of the aliphatic chains. However, in general the frustration induced by such a mismatch is solved in a tilted or helicoidal configuration. Moreover the intensity dependence measured along the difference line is inconsistent with the formation of helicoidal or zig-zag arrays but is rather compatible with the existence of antiferroelectric pairing between two neighbouring molecules along the columns (diffracted intensity in the diffuse plane in $q_0 = 2\pi/11{\cdot}2$ Å is much higher than that measured in $2q_0$).

The hypothesis of the antiferroelectric association has been confirmed by the X-ray crystal structure of the short chain derivative **1a**. The results are quite surprising. In fact, X-ray analysis shows that the molecules stack in columns (see figure 7) and form antiferroelectric pairs, probably due to antiparallel dipolar interactions. The crystallographic system is triclinic with space group P^{-1}. More details about the crystalline parameters will be discussed in a forthcoming paper.

Using the crystallographic data the dipole moment of the boat conformation of **1a** in the solid state has been evaluated by computer assisted calculation [14]. A remarkably high value of 10·3 D was obtained. This large dipole moment is probably the driving force for the antiferroelectric pairing within the columns in the solid state. Moreover the overall dipole moment of a pair has been calculated to be close to zero, indicating an almost perfect matching of the dipoles of the two molecules in the pair. Useful information on the symmetry, macroscopic alignment and dielectric properties of this new class of columnar liquid crystals have been obtained by deuterium NMR spectroscopy. The results of such studies on derivative **1e** [15] are consistent with the presence of a uniaxial columnar mesophase having a negative dielectric anisotropy, in agreement with the X-ray diffraction measurements.

FTIR measurements: infrared spectroscopy was used to investigate the conformational changes associated with the mesophase–isotropic, the C_1–mesophase and the C_2–C_1 transitions. In the interpretation of the dynamic changes involved at the phase transitions, particular effort was directed to define the conformational behaviour of the alkyl chains. The degree of disorder of the alkyl chains is associated with the presence of *trans–gauche* (*tg*) conformations, while *trans–trans* (*tt*) conformations denote a completely ordered structure [16, 17]. The survey infrared spectrum of compound **1f** in the solid form C_1 at 26°C is shown in figure 8: our interest is focused on the C=O stretching (1760–1780 cm^{-1}), CH_2 symmetric and antisymmetric stretching (3000–2800 cm^{-1}), CH_2 bending (1500–1350 cm^{-1}) and CH_2 rocking (900–700 cm^{-1}) vibrations. At 82°C (isotropic state) the lateral alkyl chains present a completely disordered conformation as demonstrated by the positions and intensities of the CH_2 rocking, bending and stretching vibrational modes. Figure 9 (*a*) shows the temperature dependence of the conformational disorder in the aliphatic part derived from the CH_2

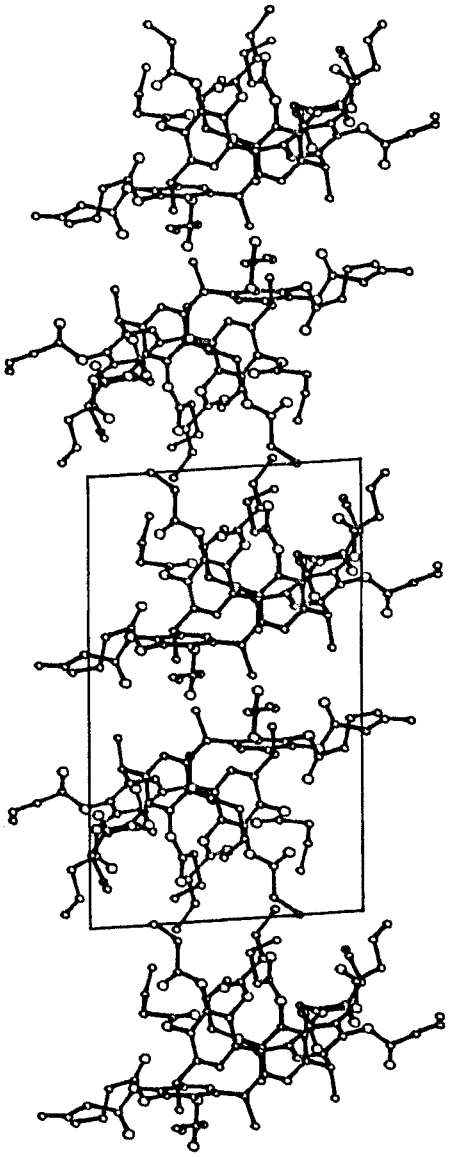

Figure 7. *Z* axis projection of **1a**, showing the columnar arrangement of antiferroelectric pairs of molecules.

rocking intensities: the mesophase–isotropic transition at 60°C is associated with a small increase of intensities of the CH_2 rocking modes, which rise continuously from 60 to 24°C, where an abrupt increase of the precited bands intensities is detected.

In the C=O stretching region the band at 1778 cm^{-1} registers a $-2\,cm^{-1}$ shift at the mesophase–isotropic transition while the shoulder at about 1760 cm^{-1} remains unvaried. Relative intensities of the two bands in C_1 have been demonstrated to depend on the cooling rate: a rapid cooling brings a larger contribution of the low frequency band.

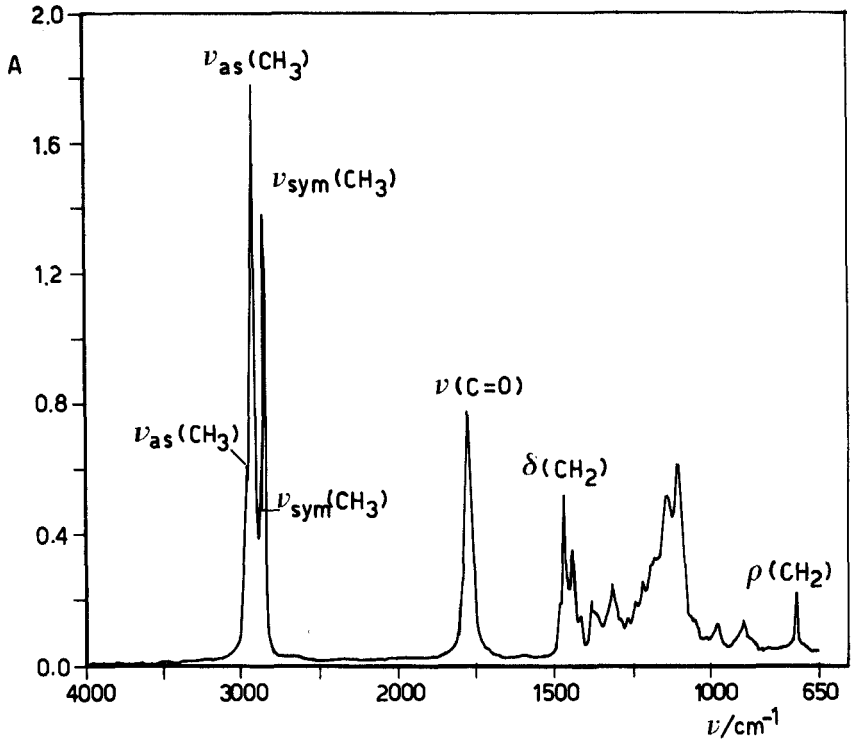

Figure 8. FTIR spectrum of compound **1f** in the solid form C_1 at 26°C.

The side chain conformational order, expressed as the *tt*/*tg* ratio, increases at every phase transition, from a completely disordered or molten conformation in the isotropic liquid to the organized *tt* situation of C_1.

3.4. C_2 *characterization: X-ray diffraction and FTIR*

As already described in § 3.2, C_1 transforms into C_2 when the sample is heated very slowly from 25 to 46°C and maintained at that temperature for 3 hours.

3.4.1. *FTIR measurements*

The first transformation is observed at 40°C and small changes in the intensities and frequencies of the CH_2 vibrational modes in the direction of the tg conformation are found. But this is only a short-lived situation because at 46°C the aliphatic chains reorganize in the *tt* conformation (see figure 9(*b*)). Other interesting changes are the down shift of the C=O stretching peak ($-4\,cm^{-1}$) and the disappearance of the shoulder. Therefore C_2 has a higher conformational order than C_1 in the aliphatic and C=O parts of the molecule.

3.4.2. *X-ray diffraction measurements*

The cell parameters for the solid form C_2 of **1f** have been obtained. The cell is orthorhombic ($a=45{\cdot}5$ Å, $b=20{\cdot}4$ Å, $c=12{\cdot}5$ Å); the organization remains columnar with correlations between neighbouring columns and with a repeat period of 12·5 Å along the columnar axis (presence of antiferroelectric pairs). Each column retains the

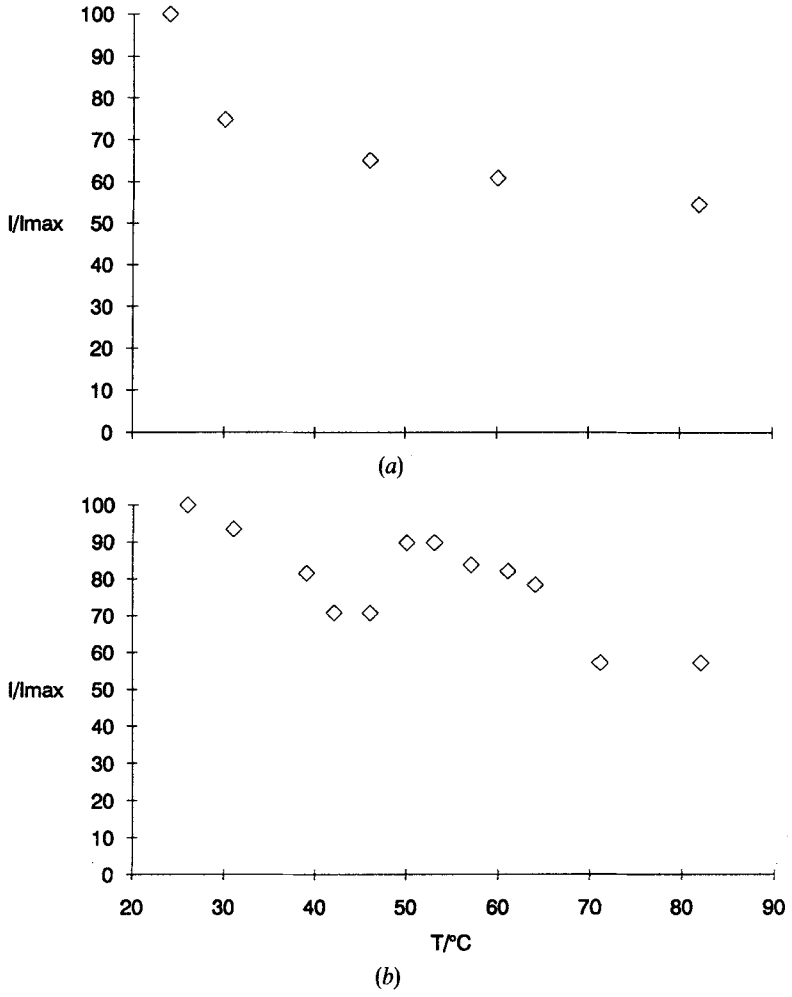

Figure 9. (*a*) Variation of the CH_2 rocking band intensities with temperature: mesophase–isotropic and C_1 mesophase transitions (cooling cycle); (*b*) variation of the CH_2 rocking band intensities with temperature: C_1–C_2 transition (heating cycle) at 46°C.

same cross section with respect to the mesophase, but the aliphatic chains are now asymmetrically distributed around the macrocyclic core.

Summarizing, C_1 has a three dimensional organization resembling the two dimensional one of the mesophase of which it is the precursor, while C_2 has a different, more stable crystal packing which, upon heating, melts directly to the isotropic liquid.

4. Conclusions

The mesomorphic properties of this new class of macrocyclic mesogens have been elucidated by means of several techniques. Alkanoyloxy derivatives **1c–g** exhibit a uniaxial columnar organization classified as D_{ho} (hexagonal columnar ordered) having negative optical and dielectric anisotropy. Both planar and homeotropic alignments have been achieved, the first by shear and the latter just by cooling from the isotropic liquid. Mesophase stability over time is related to the alkyl chain length: **1d–g** show enantiotropic mesophases and **1c** a monotropic mesophase on cooling. An

antiferroelectric pairing of the molecules within the columns is observed, caused by an almost perfect dipole matching of the molecules in each pair. Optical microscopy and DSC experiments have revealed a complex thermal behaviour for **1c–h**. Particularly interesting is the presence in all the mesogens of two solid phases C_1 and C_2 having different three dimensional organization. C_1 is the true mesophase precursor, while C_2 melts directly to the isotropic liquid. The greater viscosity of the longer chain derivatives **1e–g** increases the mesophase stability over time, by preventing the transition to C_1. C_2, the thermodynamically more stable crystal form, is obtained when the mesogens are allowed to stand in the low mesophase temperature range for some hours. Several factors contribute to the generation of such mesomorphic complexity: molecular structure, thermal history, heating–cooling scanning rates, sample thickness, etc. However, as in other non-flat discotic mesogens [18], the ultimate source of such complexity is related to the combination of the different possible core packing geometries with the numerous conformations available to the alkyl chains. For this reason the knowledge of the conformations assumed by the macrocyclic cores within the columns in the various phases would be important. FTIR and deuterium NMR studies of selected deuteriated derivatives are in progress to address it.

We thank Dr L. Longo and Dr R. Marola (Istituto Donegani, Novara, Italy) for dipole moment calculations and FTIR measurements and Dr F. Ugozzoli (University of Parma, Italy) for X-ray crystal structure determination.

References

[1] LIN LEI, 1983, *Molec. Crystals liq. Crystals*, **91**, 77.
[2] LIN LEI, 1987, *Molec. Crystals liq. Crystals*, **146**, 41.
[3] LEUNG, K. M., and LIN LEI, 1987, *Molec. Crystals liq. Crystals*, **146**, 71.
[4] MALTHÊTE, J., and COLLET, A., 1985, *Nouv. J. Chim.*, **9**, 151.
[5] ZIMMERMANN, H., POUPKO, R., LUZ, Z., and BILLARD, J., 1985, *Z. Naturf.* (*a*) **40**, 149.
[6] LEVELUT, A. M., MALTHÊTE, J., and COLLET, A., 1986, *J. Phys. Paris*, **47**, 351.
[7] POUPKO, R., LUZ, Z., SPIELBERG, N., and ZIMMERMANN, H., 1989, *J. Am. chem. Soc.*, **111**, 6094.
[8] ZIMMERMANN, H., POUPKO, R., LUZ, Z., and BILLARD, J., 1986, *Z. Naturf.* (*a*) **41**, 1137.
[9] MALTHÊTE, J., and COLLET, A., 1987, *J. Am. chem. Soc.*, **109**, 7544.
[10] COMETTI, G., DALCANALE, E., DU VOSEL, A., and LEVELUT, A. M., 1990, *J. chem. Soc. chem. Commun.*, 163.
[11] BONSIGNORE, S., COMETTI, G., DALCANALE, E., and DU VOSEL, A., 1990, *Liq. Crystals*, **8**, 639.
[12] CHANDRASEKHAR, S., SADASHIVA, B. K., SURESH, K. A., MADHUSUDANA, N. Y., KUMAR, S., SHASHIDAR, R., and VENKATESH, G., 1979, *J. Phys. Paris*, Coll. 3, C3.
[13] DE GENNES, P. G., 1983, *J. Phys. Paris*, **44**, L657.
[14] Calculated using Sybyl, a computer program by Tripos.
[15] ABIS, L., ARRIGHI, V., COMETTI, G., DALCANALE, E., and DU VOSEL, A., 1991, *Liq. Crystals*, **9**, 277.
[16] YANG, X., KARDAN, M., HSU, S. L., COLLARD, D., HEATH, R. B., and LILLYA, C. P., 1988, *J. Phys. Chem.*, **92**, 196.
[17] YANG, X., WALDMAN, D. A., HSU, S. L., NITZSCHE, S. A., THAKUR, R., COLLARD, D. M., LILLYA, C. P., and STIDHAM, H. D., 1988, *J. chem. Phys.*, **89**, 5950.
[18] MORRIS, N. L., ZIMMERMANN, R. G., JAMESON, G. B., DALZIEL, A. W., REUSS, P. M., and WEISS, R. G., 1988, *J. Am. chem. Soc.*, **110**, 2177.